

Evaluation of the Influence of The Number of Laser Shots on The Characterization of TiO₂/MgO Nanocomposites

Zainab J. Shanan*, Huda M.J. Ali, H.F. Al-Taay

* zainabjs_phys@csu.uobaghdad.edu.iq

Department of Physics, College of science for Women, University of Baghdad, Baghdad, Iraq

Received: January 2022

Revised: April 2022

Accepted: June 2022

DOI: 10.22068/ijmse.2651

Abstract: This work aims to synthesize TiO₂/MgO nanocomposites using a pulse laser deposition technique. At a vacuum pressure of 2.5×10^{-2} mBar, TiO₂/MgO nanocomposites were synthesized on substrates with a laser power of 600 mJ and a wavelength of 1064 nm. This search utilizes various pulses (500, 600, and 700) at a 6-Hertz repetition rate. X-ray diffraction was used to investigate the crystallography of the phases in the samples, as well as average crystallite size (XRD). An increase in the average crystal size was observed with an increase in the number of shots (from 35.15 to 38.08) nm at (500 to 700) shots, respectively. The impact of the number of laser shots on the surface characteristics of TiO₂/MgO nanocomposites was also evaluated using atomic force microscopy (AFM) and field emission scanning electron microscopy (FE-SEM). Finally, optical characteristics were evaluated using UV-Vis spectroscopy. Increasing the number of shots increased the absorbance and thus reduced the energy gap.

Keywords: TiO₂/MgO nanocomposites, Scan electron microscopy, PLD, X-Ray diffracting, Nd:YAG laser.

1. INTRODUCTION

Nanoparticle productions and their application areas have promising domains in science and technology in terms of unknown properties and behavior due to their size-dependent features [1]. Pulse laser deposition (PLD) is a thin film deposition technique that is becoming increasingly popular due to its low cost, ease, versatility, and capability in synthesizing high-quality films at relatively low growth temperatures. PLD has been widely used to produce stoichiometric oxide films [2, 3]. Metal oxide nanoparticles such as MgO and TiO₂ have a wide range of characteristics, which has led to their use in various applications. Titanium dioxide (TiO₂) is an essential industrial ingredient used in paint, pigments, cosmetics, and other products [4]. Because of its high dielectric constant and refractive index, it is also used in optical coatings, beam splitters, and anti-reflection coatings. It's been used as a humidity sensor and a high-temperature oxygen sensor, according to publications [4-5]. Magnesium oxide (MgO) is a versatile substance used in a variety of science and technology applications. Aside from its usage as a buffer layer in magnetic tunnel junctions, it has other applications [6]. Microelectronics, diagnostics, and bio-molecular detection are all potential uses for MgO nanoparticles [7].

The absorption of TiO₂ is limited to the UV range due to the wide bandgap (3.2 eV for anatase and 3.0 eV for rutile). For this reason, a variety of techniques have been devised, such as doping with metallic (e.g., Fe, Cr, and Mg) and non-metallic elements (e.g., N and S) into the TiO₂ lattice, which might significantly increase TiO₂ photocatalytic activity in both the UV and visible areas [8].

MgO nanostructured materials have a high melting point, chemical stability, electric resistivity, and thermal expansion coefficient. TiO₂ nanostructured materials, on the other hand, have excellent optical, electrical, dielectric, and catalytic characteristics. As a high-temperature insulator and optoelectronic device, MgO and TiO₂ nanostructured materials were employed [9, 10]. Metal oxide nanocomposite materials constructed of MgO/TiO₂ have a wide range of applications in the electronics area. Different shapes such as nano tubes, nano rods, nano belts, and nano dots were created by combining the various materials [11, 12]. The qualities of qualities of thin films are primarily determined by the procedures used to create them. Various methods have been used to produce TiO₂/MgO nanostructures, including sol-gel method [13, 14], a one-step sintering technique [15], mechanical activation [9], microwave-assisted method [16], and pulse laser technique [17]. The PLD

technique was used to produce TiO₂/MgO films in this paper. Because the reactant formulas are comparable, laser deposition of pulses that are suited for the removal of complicated oxides can be improved. High-energy laser pulses are utilized in PLD technique to vaporize the substance from the target surface because the ambient pressure combination in the deposit chamber is very low and the radiation signal is very high in energy [18, 19].

The Nd: YAG laser is one of the solid-state lasers utilized in deposition technologies [20]. The laser (Nd: YAG) generates high-energy laser shots which are activated by the real age of electrons at a variable energy level. The active media in this situation is a high-energy repository. [21]. The laser light should be absorbed until it may affect the object. Absorption is a significant source of energy within the material. According to this source, the irradiation of Laser energy is determined by the released Laser beam [22]. This work aims to verify the creation of nanocomposites and study the impact of the number of laser shots on the physical properties of the prepared films.

2. EXPERIMENTAL PROCEDURE

2.1. Preparation

Pulsed laser deposition technique was used to prepare TiO₂/MgO nanocomposites thin film with a ratio of 1 wt% for MgO (99% Sigma-Aldrich) and TiO₂ (purity 99.8%) on glass substrates. Using a hydraulic piston, the mixtures were compressed into a 25 mm diameter, 4 mm thick pellet at a pressure of 7 tons for (10) minutes. In the Nd:YAG excimer laser (10 ns, 6 Hz), the energy was 500, 600, and 700 mJ. The No. of shots equal was 600 pulses. The TiO₂/MgO nanocomposites thin film was grown on glass. Ethanol and ultrasound were used to clean the substrates. The final stage in nanocomposite film preparation is to anneal thin films at 450°C for (1 h).

2.2. Characterization

Samples were characterized with X-ray diffraction using (Philips PW), the target CuK α radiation, wavelength λ (1.5406 Å) at a voltage (40.0 kV), current (30.0 mA), and scan range: 10.00- 80.00 (deg) to the X-ray tube. The topography of the surface was examined using atomic force microscopy (AFM), SPM (Model AA3000), and tip

NSC35/AIBS from Angstrom Advanced Inc (USA) was used to determine the nanocrystalline topography. The morphology of the surface (shape and particle size) was examined via field emission scanning electron microscopy (FESEM) Using a MIRA3 TESCAN Mashhad (MUMS) model. The optical transmission measurements were obtained using UV-Vis spectrophotometer, SP-3000 plus, OPTIMA INC. Japan.

3. RESULTS AND DISCUSSIONS

3.1. X- Ray Diffraction Analysis

The structural phase for the TiO₂/MgO nanocomposites films deposited on glass substrate at different no. of pulses was confirmed by the X-ray diffraction pattern. The patterns of XRD were shown in Fig. (1). The agreement between XRD structure for all TiO₂, and MgO NPs samples and JCPDS standard card No. 00-004-0551, and 00-045-0946, respectively, which exhibits structure with rutile TiO₂ phase and cubic phase for MgO is shown in Fig. (1). The larger the number of shots, the best the crystallization and growth of peaks; this also suggests that as-prepared films have polycrystalline structure attributed to the prevalence of multiple peak inclinations.

The existence of nanostructure is shown by the widening of the diffraction pattern in the X-ray spectra. The crystal size was calculated using the Debye-Scherrer formula [18].

$$C.S = k\lambda / \beta \cos\theta \quad (1)$$

Where (CS) denotes the crystalline size, (θ) the diffraction peak degree, (λ) the wavelength of X-ray, and (β) the full peak width at half maximum (FWHM). With an increase in the number of pulses, the crystal size increased, which can be attributed to enhanced crystallization in the produced films. The current study's findings contradict the findings of the reference [23].

To have information on the number of imperfections in the films, the dislocation density (δ) was calculated using the formula [24].

$$\delta = 1 / (C.S)^2 \quad (2)$$

Where CS is the crystallite size, the number of dislocations intersecting a unit area of a random section, is defined as this quantity. It is shown from Table 1 that the δ value of the preferential orientation of the XRD peaks along the (110) direction is smaller than the other peaks in all samples.

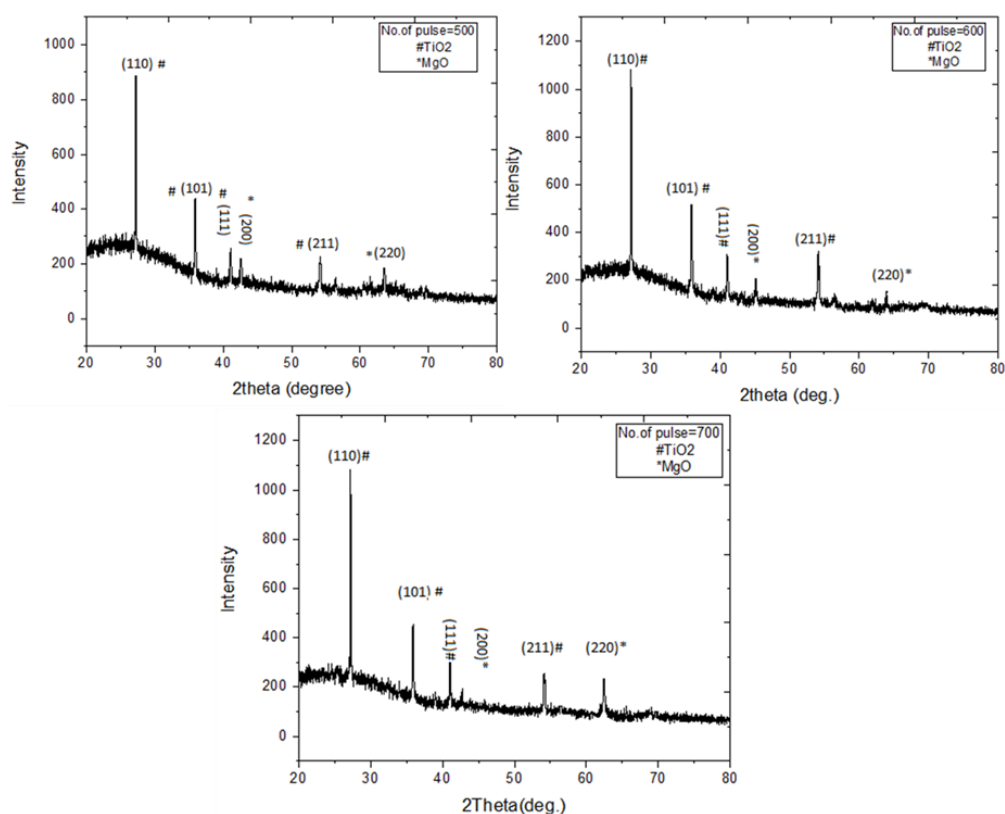


Fig. 1. XRD spectra of the TiO₂/MgO nanocomposite at variable of laser shots.

Table 1. The diffraction angle (2θ), interplaner distance (d), FWHM (β), the miller indices, the crystallite size (CS), and the dislocation density (δ) of TiO₂/MgO films.

No. of Pulses Laser	2θ (Deg.)	d(Å)	FWHM (Deg.)	hkl	Phase	CS (nm)	δx10 ⁻⁴ (nm ⁻²)	Average CS (nm)
500	27.22	3.27	0.14	(110)	RutileTiO ₂	56.76	3.10	35.15
	35.88	2.50	0.19	(101)	RutileTiO ₂	43.94	5.18	
	41.04	2.19	0.26	(111)	RutileTiO ₂	32.00	9.76	
	42.70	2.11	0.31	(200)	Cubic MgO	27.075	13.64	
	54.13	1.69	0.27	(211)	RutileTiO ₂	33.04	9.16	
	62.76	1.47	0.51	(220)	Cubic MgO	18.06	30.63	
600	27.21	3.27	0.147	(110)	RutileTiO ₂	55.60	3.23	36.91
	35.89	2.49	0.184	(101)	RutileTiO ₂	45.38	4.86	
	41.03	2.19	0.225	(111)	RutileTiO ₂	37.69	7.03	
	43.93	2.05	0.305	(200)	Cubic MgO	28.09	12.67	
	54.10	1.69	0.278	(211)	RutileTiO ₂	32.08	9.71	
	62.64	1.48	0.411	(220)	Cubic MgO	22.62	19.53	
700	27.24	3.27	0.156	(110)	RutileTiO ₂	52.39	3.64	38.04
	35.90	2.49	0.198	(101)	RutileTiO ₂	42.17	5.62	
	41.04	2.19	0.242	(111)	RutileTiO ₂	35.05	8.14	
	43.87	2.06	0.246	(200)	Cubic MgO	34.81	8.25	
	54.13	1.69	0.273	(211)	RutileTiO ₂	32.67	9.36	
	62.64	1.48	0.299	(220)	Cubic MgO	31.31	10.34	

This may be due to an increase in crystallization in this direction, as increasing crystallization leads to a decrease in dislocations and defects. The variation in CS and dhkl values may be associated with different factors such as surface defects, strain, and dislocations [25]. In other words, the decrease in crystallin size (CS) corresponds to an increase in the dislocation density (δ) values [24]. Table 1 shows the change in crystallite size for different numbers of laser pulses for TiO₂/MgO thin films and other XRD parameters.

3.2. Surface Morphological Studies

Atomic Force Microscopy (AFM) is a surface analysis technique that captures high-resolution images of a surface to obtain microscopic information on the surface structure and plot topographies that depict surface relief. The grain size and surface roughness of TiO₂/MgO nanocomposites thin films were evaluated using AFM. The AFM images of as-deposited at different numbers of shots (500-700) with two and three dimensions are shown in Fig. (2).

AFM analysis of the TiO₂/MgO samples revealed that the number of shots significantly impacts their surface morphologies. The thin films as observable in the images are made of aggregates (clusters) with a spherical grain. Also, the surface roughness of TiO₂/MgO films has been studied by AFM. The calculated average grain size, root mean square roughness (Rq), and average roughness (Ra) of the films are listed in Table 2. Table 2 demonstrates when the number of shots increases from 500 to 700; surface roughness increases from 0.75 to 1.17 nm, resulting in a rise in grain size from 50.45 to 78.33 nm. The roughness of the films is inevitable because the granules are spherical and of different sizes. It is also believed that the surface roughness of the film is mostly caused by the surface morphology of the glass substrate.

3.3. Field Emission- Scan Electron Microscopy Analysis (FE-SEM)

The microstructural evolution and chemical composition of different elements present in MgO/TiO₂ nanocomposite samples was studied by FE-SEM, and EDX as shown in Fig. (3). By analyzing the images of FE-SEM, it is shown that all the fabricated TiO₂/MgO nanocomposites were almost spherical with some agglomeration observed so that they were aggregated and shaped as irregular grains. Fig. (3) also showed that the average particle size increases from 21.64 nm to 37.14 nm as the number of shots increases from 500 to 700, consistent with the XRD and AFM analyses. This increase may be attributed to a thickening of the material as the number of pulses increases. These findings agree with those of X-ray diffraction and atomic force microscopy.

Energy-dispersive X-ray spectroscopy from the complete FESEM scanned region of thin films, as shown in Fig. (4), verifies the presence of Ti, O, and Mg elements in the thin films.

In addition, the scan gave information on the proportion by weight (wt %) of each element present, indicating that these prepared thin films contain specific stoichiometric amounts of TiO, MgO, and O, as can be seen in Fig.(4).

3.4. Optical Properties

Fig. (5) depicts UV-Vis absorption spectra of TiO₂/MgO nanocomposite films with varying pulses; the absorption spectrum shifts to visible light as the thin film thickness increases. Transmittance decreases at wavelengths with high absorption and increases at wavelengths with low absorption, as seen in Fig. (6).

For high photon energy, the absorption edge was calculated from the 'Tauc's formula [26]

$$(\alpha h\nu) = A (h\nu - E_g)^n \quad (3)$$

where A is a constant, α (cm⁻¹) is the absorption coefficient, and $h\nu$ (eV) is the energy of

Table 2. average grain size, root mean square (RMS) and roughness for TiO₂/MgO Nanocomposite

No. of pulses Laser	Average grain size (nm)	(RMS) (nm)	roughness (nm)
500	50.45	0.86	0.75
600	53.46	1.16	0.97
700	78.33	1.37	1.17

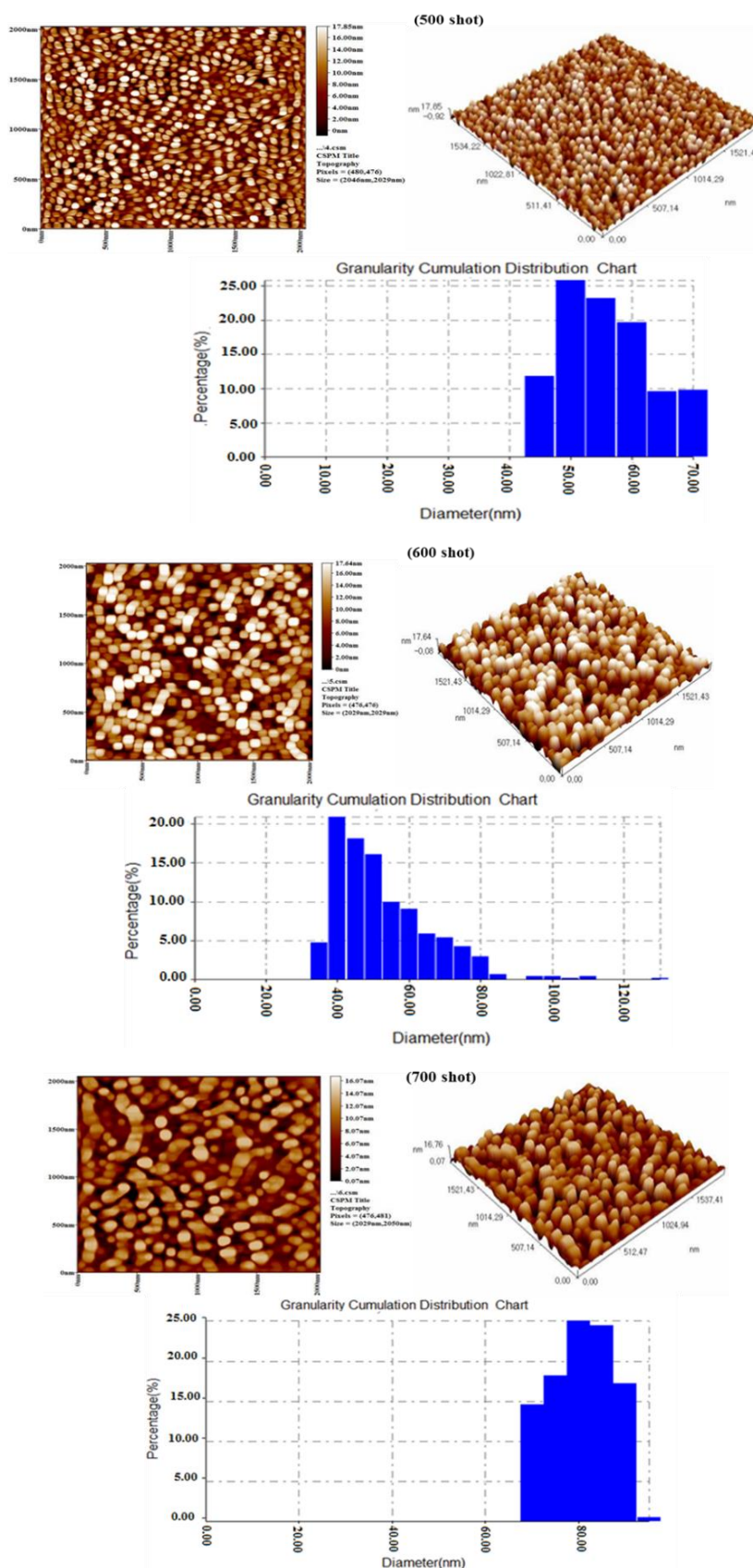
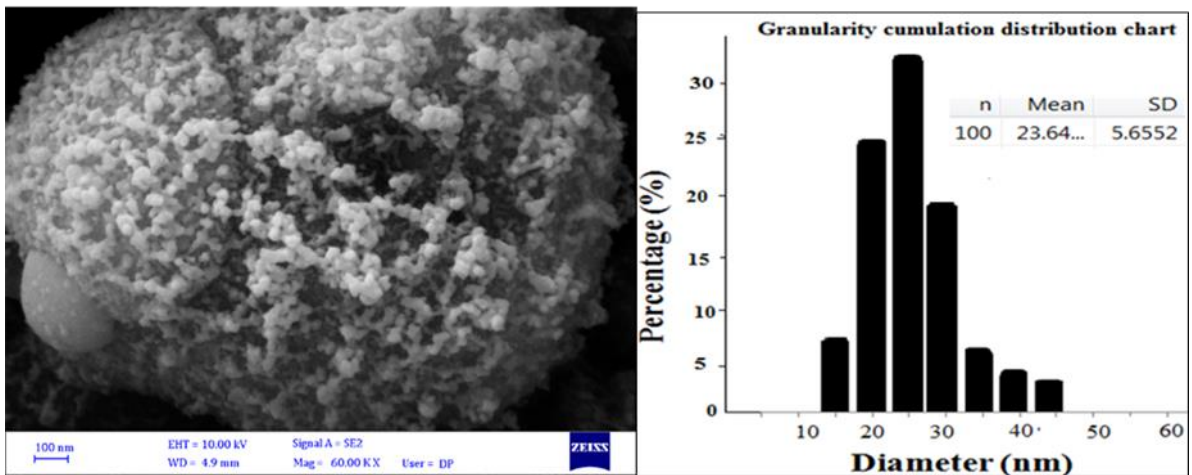
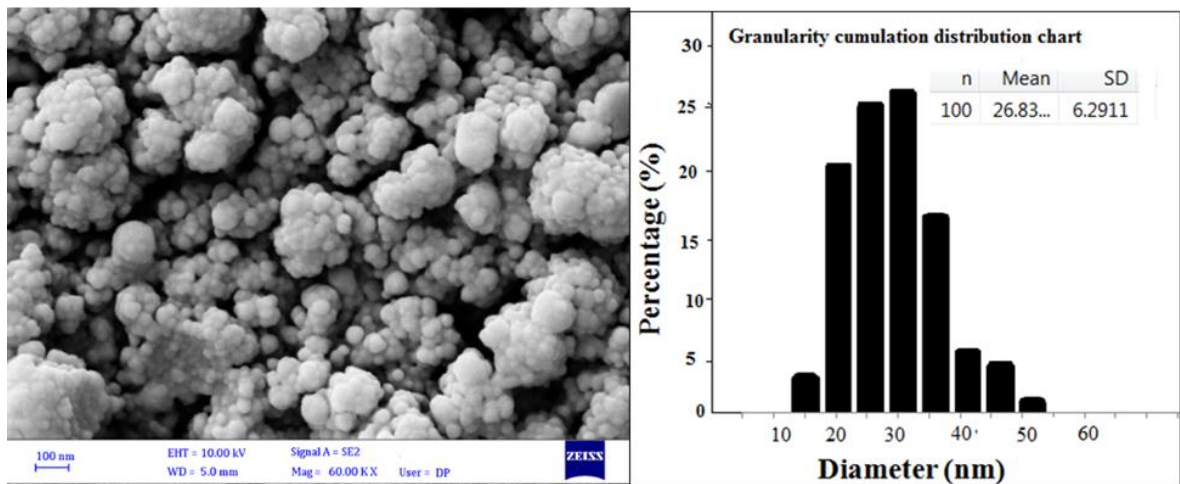


Fig. 2. (3D), (2D) AFM images and Granularity on. of distribution for TiO₂/MgO nanocomposites at various numbers of laser shots.

(500 shot)



(600 shot)



(700 shot)

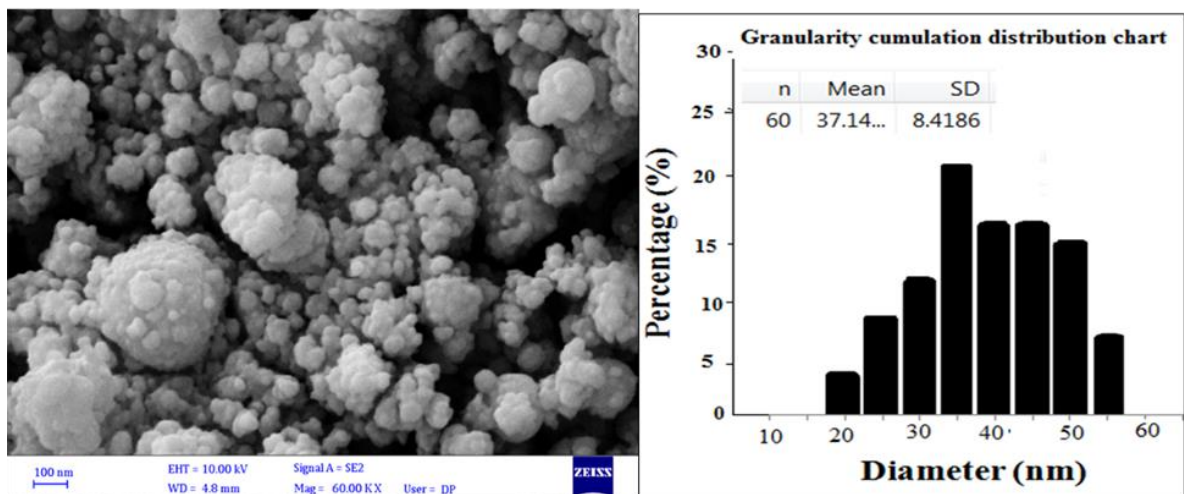


Fig. 3. Field emission scan electron microscopy images, and particle size distribution histogram for synthesized TiO_2/MgO Nanocomposite at various numbers of laser shots.

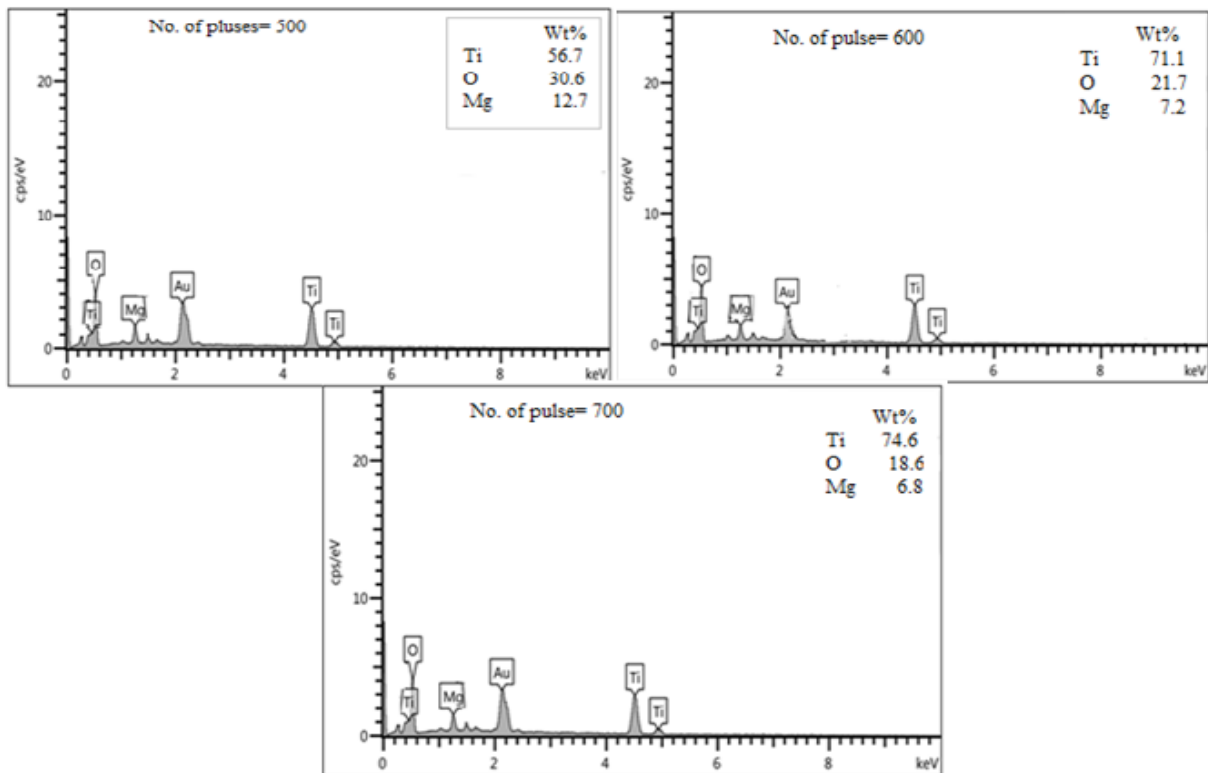


Fig. 4. EDX analysis of prepared TiO₂/MgO nanocomposite at various numbers of laser shots.

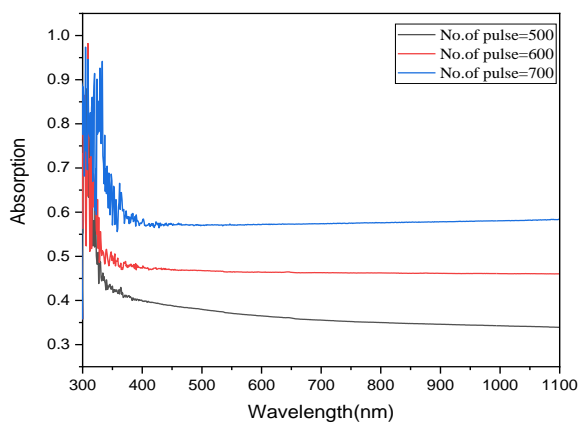


Fig. 5. Absorption of the TiO₂/MgO nanocomposite at various numbers of laser shots.

excitation, where n is (0.5) for a direct transition semiconductor and (2.0) for an indirect transition semiconductor. The $(\alpha h\nu)^2$ (or 0.5) vs. $(h\nu)$ plot, which was used to measure the band gap energy, revealed better linearity in the entire absorption area, supposing the absorption coefficient matching to the band gap energy. Band gaps energy of TiO₂/MgO films were estimated to be (3.5, 3.2, and 2.9) eV at No. of shot (500, 600,

700), respectively, as noted in Fig. (7). These results are consistent with the increased particle size.

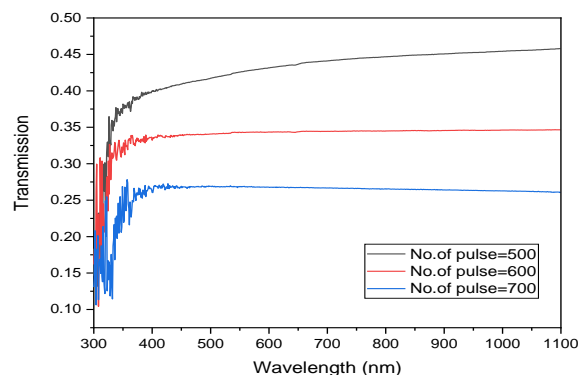


Fig. 6. Transmittance of the TiO₂/MgO nanocomposite at variable of laser shots.

Increasing the thickness of the samples led to a decrease in the energy band gap with an increase in the number of laser pulses, which is associated with increased localized energy levels between the conduction and valence bands, leading to increased absorption; these results are consistent with previous work [23].

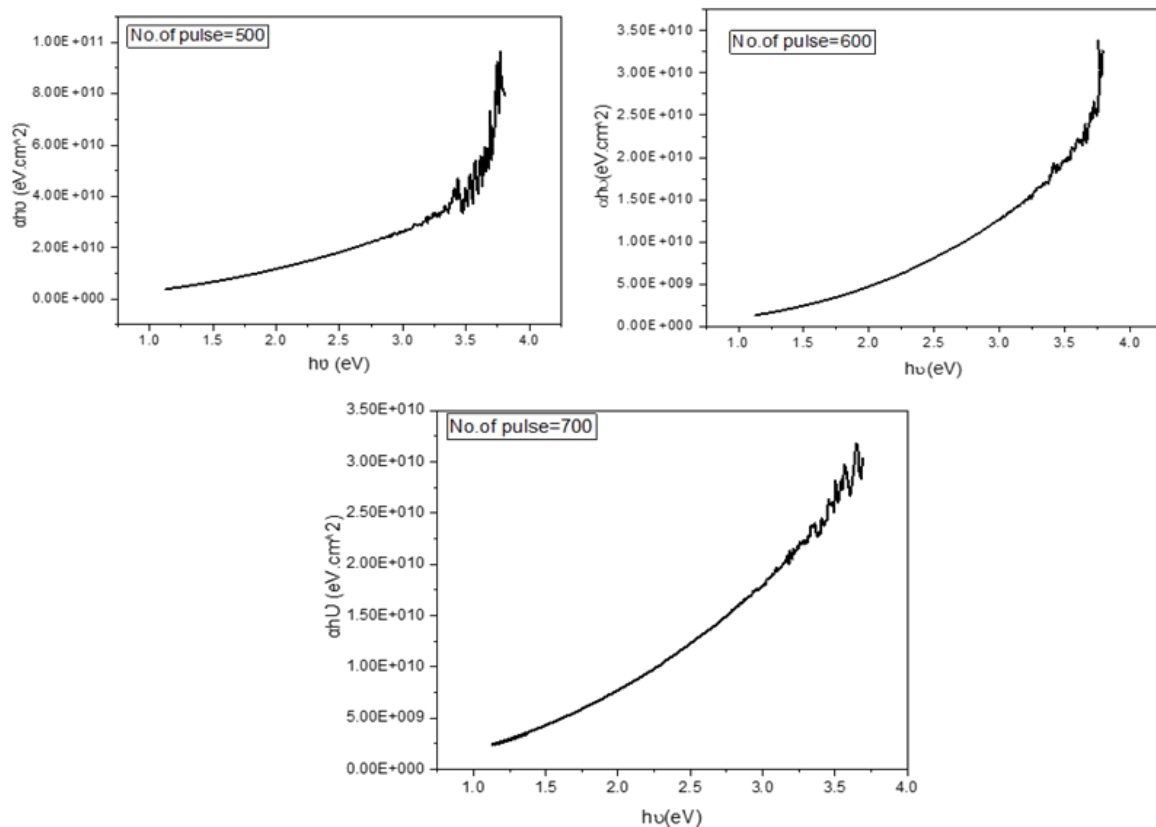


Fig. 7. Optical energy gap of the TiO₂/MgO nanocomposite at various numbers of laser shots.

On the other hand, this decrease can be attributed to the apparent increase in the number of photons that collide with the material due to the increase in the number of laser pulses, which causes the material to absorb more photons. This reduces the energy gap by increasing the number of electrons and holes. The regulation of atom distribution inside the material and the modification of

crystalline phases, as well as the type of matter by modifying the deposition energy, all contribute to this decrease in the energy gap value [19].

Fig. (8) depicts the relationship between crystal size and energy gap with the number of laser pulses for the prepared films, demonstrating that the larger the crystal size, the smaller the energy gap.

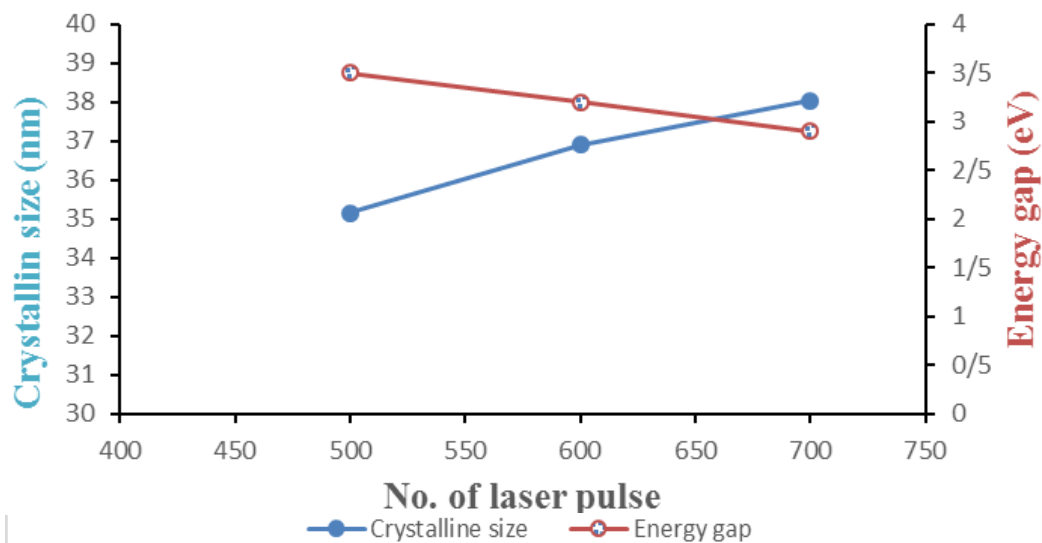


Fig. 8. The variation of crystal size and energy gap with numbers of laser shots for TiO₂/MgO nanocomposite.

4. CONCLUSIONS

PLD procedure can be used to produce thin films that are efficient and rapid, as well as being an inexpensive technology. It can be observed that when No. of laser shots increases, the size of crystals increases with the stability of other laser parameters. With more shots, the surface roughness and grain size also increase as the thickness increases, and the surface roughness and grain size increase. Morphologies of the particles were almost spherical, with some agglomeration, indicating that they were aggregated and formed as irregular granules, according to FESEM data. Moreover, it is clear from the results of the experiment examination (UV) that with an increase in no. of shots, there is an increase in absorbance. However, the energy gap reduces with the increase in no. of pulses.

REFERENCES

- [1] Al-Nassam, S. I., Hussein, F. I., and Ma, A. K., "The effect of laser pulse energy on ZnO nanoparticles formation by liquid phase pulsed laser ablation". *J. Mater. Res. Technol.*, 2019, 8, 4026–4031. doi: 10.1016/j.jmrt.2019.07.012.
- [2] Esraa, K. H., Farah, H., and Makram, F., "Laser wavelength and energy effect on optical and structure properties for nano titanium oxide prepared by pulsed laser deposition." *Iraqi J. Sci.*, 2014, 12, 62-68.
- [3] Simon, N. O., Odireleng, M. N. and Hendrik, C. S., "Latest Development on Pulsed Laser Deposited Thin Films for Advanced Luminescence Applications." *Coatings*, 2020, 10, 1078. doi:10.3390/coatings10111078.
- [4] Mangrola, M. H, Parmar, B. H., Pillai, A. S., and Joshi, V. G., "Structural , Optical and Electrical Properties of Titanium Dioxide Nanoparticles." *Multi Disciplinary Edu Global Quest* , 2012, 1, 138–145.
- [5] Dhage, S. R., Gaikwad, S. P., and Ravi, V., "Synthesis of nanocrystalline TiO₂ by tartarate gel method." *Bull. Mater. Sci.*, 2004, .27, 487–489. doi: 10.1007/BF02707273.
- [6] Sinha, M., Gupta, R. K., Dasilva, P., Mercere, P., and Modi, M. H., "Modification of optical properties of magnesium oxide (MgO) thin film under the influence of ambience." *Proceedings of the American Institute of Physics Conf.*, 2020, 1-4.
- [7] Rand, A., Shanan. Zainab, J. Sh., Ghada, M., S., and Quraysh, A., "Green synthesis and the study of some physical properties of MgO nanoparticles and their antibacterial activity." *Iraqi J. Sci.*, 2020, 61, 266–276.
- [8] Meng, F., Dehouche, Z., Nutasarin, A., and Fern, G., R, "Effective MgO-doped TiO₂ nanoaerogel coating for crystalline silicon solar cells improvement." *Int. J. Energy Res.*, 2018, 42, 3915–3927.
- [9] Filipovic, S. D. A, Obradovic, N., Kosanovic, D., Pavlovic, V., "Sintering of mechanically activated MgO-TiO₂ system," *J. Ceram. Process. Res.*, 2015, 14, 31-34.
- [10] Lopez, T., Hernandez-Ventura, J., Aguilar, D. H., and Quinana, P., "Thermal phase stability and catalytic properties of nanostructured TiO₂-MgO sol-gel mixed oxides." *J. Nanosci. Nanotechnol.*, 2008., 8, 6608–6617.
- [11] Photiphitak, C., Rakkwamsuk, P., Muthitamongkol P., Thanachayanont, C., "Performance Enhancement of Dye-Sensitized Solar Cells by MgO Coating on TiO₂ Electrodes." *World Academy of Science, Engineering and Technology*, 2012, 6, 463-467.
- [12] Lopez, T., Hernandez, J., Gomez, R., Bokhimi X., Boldu, JL., "Synthesis and Characterization of TiO₂-MgO Mixed Oxides Prepared by the Sol-Gel." *Langmuir*, 1999, 15, 5689-5693.
- [13] Mursal, Ismail, Viza, Y., and Evi. Y., ""Structural and optical properties of MgO-doped TiO₂ prepared by sol-gel method". *Proceedings of the American Institute of Physics Conf.* 2221, 1-7.
- [14] Hasan, A. H., "Study the structural and optical properties of titanium oxide thin film, doped with chromium prepared in Sol-Gel method." *Iraqi J. Phys.*, 2019, 16, 64–70.
- [15] Waiwong, R., Ananta, S., and Pisitanusorn, A., "Influence of the MgO-TiO₂ co-additive content on the phase formation,

- microstructure and fracture toughness of MgO-TiO₂-reinforced dental porcelain nanocomposites.," J. Korean Ceram. Soc., 2017, 54, 141–149.
- [16] Glisenti, A., Frasson, A., Galenda, A., Ferroni, M., Concina, I., and Natilea, M. M., "Synthesis and characterization of Ag/CeO₂ nanocomposites.", Mater. Res. Soc. Symp. Proc., 2010, 1257, 323–328,
- [17] Obeid, B. G., Hameed, A. S., and Alaaraji, H. H., "Structural and optical properties of TiO₂: MgO thin films preparing at 373K.", Dig. J. Nanomater. Biostructures, 2017, 12, 1239–1246.
- [18] Lanje, A. S., Sharma, S. J., and Pode, R. B., "Synthesis and Characterization of Copper Oxide Nanoparticles.", Int. J. Adv. Eng. Res. Dev., 2017, 04. doi: 10.21090/ijaerd.ncn01.
- [19] Zainab, J. Sh., Mirvat, D. M. and Kadhim, A. A., "Impact the number of pulse laser on the physical properties of ZnO/CuO nano structure", Proc. III Int. Conf. Adv. Technol. Mater. Sci. Mech. Autom. Eng. MIP Eng. – 2021, 2402, no. 130005.
- [20] Maxim, V. Bogdanovich, Vladimir, V. Kabanov, Gennadii, I. Ryabtsev, Andrew, G. Ryabtsev, Yahor, V. Lebiadok , "High-performance LD-pumped solid-state lasers for range finding and spectroscopy ", Proceedings of SPIE - The International Society for Optical Engineering 2012, 86770X-1-86770X-6.
- [21] Kosti, S., Lazarevi, Z.Ž., Radojevi, V., Milutinovi, A, Romcevi. M, Romcevi, N.Ž., Valci, A. "Study of structural and optical properties of YAG and Nd:YAG single crystals.", Materials Research Bulletin, 2015, 63, 80–87.
- [22] Eason, R., Pulsed Laser Deposition of Thin Films. John Wiley & Sons, Inc., 2007
- [23] Mousa, M. A. Al-M., Amer Al-N., Ghaleb Al-D. "Studying the effect of the number of laser pulses on the structure, morphology, and optical properties for a thin film of GO-Ag nanocomposites.", J. Phys.: Conf. Ser., 2021, 1999, 012141.
- [24] Dhupar, A., Kumar, S., Sharma, V., " Mixed structure Zn(S, O) nanoparticles: Synthesis and characterization", M. Sci. Pol., 2019, 37, 230-237.
- [25] KUMAR, S., SHARMA, P., SHARMA, V., " CdS Nanopowder and Nanofilm: Simultaneous Synthesis and Structural Analysis", Electron Mater. Letters, 2013, 9, 371-374.
- [26] Souheila, H., Abdelouahab, O., Saâd, R., Ouarda, B., Aicha, K., and Mostefa, S., "Effect of the Number of Dips on the Properties of Copper Oxide Thin Films Deposited by Sol-Gel Dip-coating Technique.", Iran. J. of M. Sci. and Eng., 2020, 19, 1-8.